

Composite Rigid-Foldable Curved Origami Structure

Tomohiro Tachi

Assistant Professor, The University of Tokyo, Tokyo, Japan, *tachi@idea.c.u-tokyo.ac.jp*

Summary: In this study, we show a family of multilayered rigid-foldable and flat-foldable vault structures. A vault can be designed by constructing a rigid-foldable curved folded tubular arch and assembling the arches to construct a multilayered surface. The resulting vault is also rigidly flat-foldable. We first show the process involved in the geometric construction of the tubular structure from a given space curve defined by curvature and torsion functions. Next, we show a single-DOF rigid-folding motion that is enabled by the curved folded tube. Finally, we show the parametric design of a vault structure and discuss its design parameters and the resulting form.

Keywords: *Deployable Structure, Rigid Origami, Curved Folding*

INTRODUCTION

Rigid-foldable origami, a mechanism comprising rigid panels and hinges, can be used for designing deployable shells. For large-scale implementation of such a mechanism, it is important to consider the thickness, not only that of a single panel but also the total depth of composite structures to increase the structure's stiffness and insulate the interior from heat and sound. A general method for adding thickness to panels of rigid origami [1] involves a tradeoff between the thickness of panels and the maximum fold angles; thus, the structure cannot be folded compactly when the panels are thick. An alternative approach is to construct a tessellation of cellular structures comprising thin panels and thereby acquire virtual thickness. This approach allows efficient compact folding in a continuous one-DOF motion. To achieve this, the overall structure must be carefully designed such that it maintains the mechanism to continuously fold flat. Symmetric cylindrical rigid-foldable modules have been used to construct a cellular structure in [2]. However, in the previous studies, there were problems in the design and construction processes: (1) design variations relied on translational symmetry, and (2) the number of panels tends to be very large.

In this study, we solve these two problems by assembling rigid-foldable flat-foldable cylindrical structures using curved folding, a developable surface with smoothly curved creases. Unlike ordinary polyhedral origami, curved folding uses the bending of the surface for form development. As a result, the number of foldlines is reduced, making the folding-based fabrication easier while keeping the resulting 3D form complex and rich.

The design process is based on the method proposed in [3]. We generate a family of tubular structures from a common space curve so that they rigidly fold consistently even as they are assembled. In this study, we extend the method to smooth curved folding without tiny rigid panels, to improve constructability. The contributions of this study include (1) the use of a tube for the construction module for avoiding any unwanted kinematic flexibility

of smooth curved folding, and (2) the geometric consideration of the change in the proportion of the tube's section leading to the parametric design of the vault structure with different section curves.

First, we review the geometric construction of the folding structure generated from a space curve and discuss its kinematics in a cylindrical form. Next, we show the parametric design of the assembled vault and discuss the morphological characteristics related to its design parameters.

GEOMETRIC CONSTRUCTION

Single Curved Folding

First, we review the basic geometry of the curved folding structure generated from a space curve. Consider a generic space curve $\mathbf{x}(s)$ defined by the boundary conditions $\mathbf{x}(0)$ and $\mathbf{x}'(0)$ and its curvature and torsion functions $\kappa(s)$ and $\tau(s)$, respectively, where s parameterizes the space curve by its arc length. Next, we obtain a valid continuous Frenet–Serret frame composed of tangent, normal, and binormal vectors $\{\mathbf{T}(s), \mathbf{N}(s), \mathbf{B}(s)\} = \{\mathbf{x}'(s), \mathbf{x}''(s)/\kappa, \mathbf{x}'(s) \times \mathbf{x}''(s)/\kappa\}$ by integrating the curvature and torsion functions using the Frenet–Serret formula.

$$\begin{bmatrix} \mathbf{T}'(s) \\ \mathbf{N}'(s) \\ \mathbf{B}'(s) \end{bmatrix} = \begin{bmatrix} 0 & \kappa(s) & 0 \\ -\kappa(s) & 0 & \tau(s) \\ 0 & -\tau(s) & 0 \end{bmatrix} \begin{bmatrix} \mathbf{T}(s) \\ \mathbf{N}(s) \\ \mathbf{B}(s) \end{bmatrix}. \quad (1)$$

It is known that if a continuous valid frame is defined, we can construct a curved folding whose crease lies on the space curve (Fig. 01). We can find design examples in early computer graphics shading images by Resch [4].



Fig. 01. Space curve and curved folding.

A variety of curved folded surfaces can be constructed from the same space curve. By defining the folding angle along the curve denoted by $2\alpha(s)$, we can uniquely determine the folded surface attached to the curve. Here, $\alpha(s)$ is calculated as the angle from the osculating plane facing the binormal vector $\mathbf{B}(s)$ (Fig. 02) to the tangent plane of the surface. The geometric relationship between the curves and the angles are summarized by the following equations, as investigated by Fuchs and Tabachnikov [5].

$$\kappa(s) \cos \alpha(s) = \kappa_{2D}(s), \quad (2)$$

$$\frac{\alpha'(s)}{\tan \alpha(s)} = \frac{1}{2} \kappa_{2D}(s) (\cot \beta_L(s) - \cot \beta_R(s)), \quad (3)$$

$$\frac{\tau(s)}{\tan \alpha(s)} = -\frac{1}{2} \kappa_{2D}(s) (\cot \beta_L(s) + \cot \beta_R(s)), \quad (4)$$

where the curvature of the crease in the crease pattern is denoted by $\kappa_{2D}(s)$ and the angles between the tangent and the rulings of the two surfaces are denoted by $\beta_L(s)$ and $\beta_R(s)$, respectively.

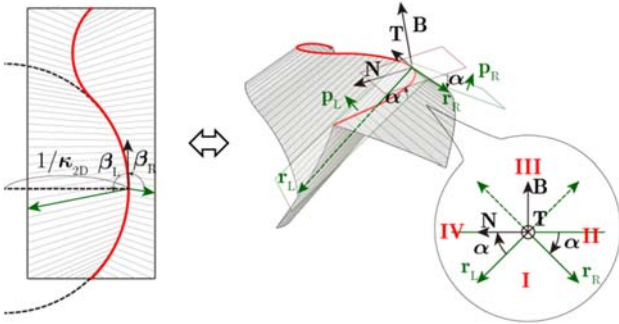


Fig. 02. Parameters (Left: Crease pattern, Right: Folded form in perspective and orthogonal projection along vector \mathbf{T}).

Therefore, the ruling vectors are described as follows:

$$\mathbf{r}_L = \cos \beta_L \mathbf{T} + \sin \beta_L \cos \alpha \mathbf{N} + \sin \beta_L \sin \alpha \mathbf{B}, \quad (5)$$

$$\mathbf{r}_R = \cos \beta_R \mathbf{T} - \sin \beta_R \cos \alpha \mathbf{N} + \sin \beta_R \sin \alpha \mathbf{B}. \quad (6)$$

The normal vectors of the surfaces are represented as follows:

$$\mathbf{p}_L = -\sin \alpha \mathbf{N} + \cos \alpha \mathbf{B}, \quad (7)$$

$$\mathbf{p}_R = \sin \alpha \mathbf{N} + \cos \alpha \mathbf{B}. \quad (8)$$

Here, four types of geometrically equivalent creased surfaces can be constructed from the same space curve and the set of ruling vectors, by choosing one from the four quadrants obtained by extending the ruling vectors in both positive and negative directions (Fig. 02). From the

first (L+R+) or third (L-R-) quadrants, a curved folding, i.e., a developable creased surface, can be constructed. From the second (L-R+) or fourth (L+R-) quadrants, a curved seam, i.e., a flat-foldable creased surface constructed from a two-ply sheet welded at the curve, can be obtained.

Modular Tube

The tubular and cellular structures are constructed in the following manner. First, we calculate a curved folding in the first quadrant (L+R+) with the constant folding angle ($2\alpha(s) = \text{const.} \in (0, 180^\circ)$) from a given space curve. At the constant folding angle, the crease pattern is characterized by the reflecting ruling lines forming angles with the curved crease ($\beta_L(s) = \beta_R(s) = \beta(s)$).

$$\cot \beta_L(s) = \cot \beta_R(s) = \frac{-\tau(s)}{\kappa_{2D}(s) \tan \alpha(s)}. \quad (9)$$

Next, we draw another curve on one side (say, the right-hand side) of the attached surfaces such that the corresponding tangent vectors of curves 1 (the original curve) and 2 (the new curve) are parallel (Fig. 03). The correspondence between the arc length parameters of these curves sharing the common ruling line is described by $s_1(t)$ and $s_2(t)$, respectively, using a common parameter $t \in [0, 1]$. The curves satisfy $\mathbf{T}_1(s_1(t)) \equiv \mathbf{T}_2(s_2(t))$, where the tangent vector in curve i is denoted by \mathbf{T}_i . Here, $s_i(0) = 0$ and $s_i(1)$ equals the length of curve i . This construction ensures that curves 1 and 2 have the same frame of $\{\mathbf{T}, \mathbf{N}, \mathbf{B}\}$ at the corresponding positions $s_1(t)$ and $s_2(t)$, respectively. The new curve is uniquely determined if its endpoint is fixed. Here, the width between the curves at $t = 0$ is denoted by $w_{12}|_{t=0} = \ell_{12}|_{t=0} \sin \beta_R$, where ℓ_{12} is the length of the ruling line between curves 1 and 2.

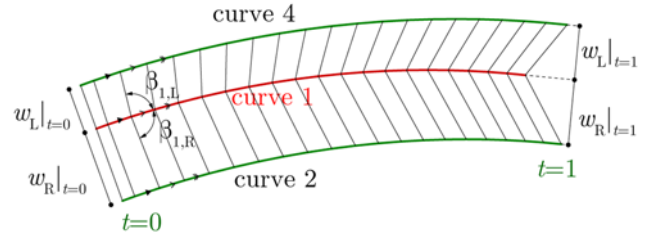


Fig. 03. Construction of curves 2 and 4, indicating the change in the proportion.

From the derived curve, we build a curved unfolding in the second quadrant (L+R-) using the same folding angle α . Because the two curves share the same frame, they also share the same ruling vectors, $\mathbf{r}_{1,R}(t) = \mathbf{r}_{2,R}(t)$ and $\mathbf{r}_{1,L}(t) = \mathbf{r}_{2,L}(t)$. This ensures that the generated surfaces overlap the right-hand side of the previous crease to form a valid two-crease surface (Fig. 04).

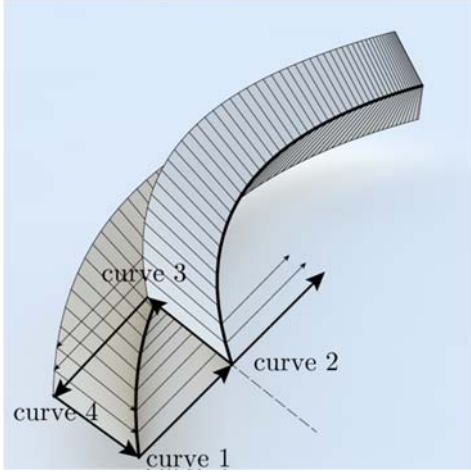


Fig. 04. Construction of the tube.

We continue constructing curves from the previously derived surfaces in the same manner, choosing the third quadrant (L- R-) and, thereafter, the fourth quadrant (L- R+). Here, we choose

$$\begin{aligned} w_{23}|_{t=0} &= w_{45}|_{t=0} = w_L|_{t=0}, \\ w_{12}|_{t=0} &= w_{34}|_{t=0} = w_R|_{t=0}, \end{aligned} \quad (10)$$

so that curves 5 and 1 lie on each other to form a valid tubular surface. Equation (10) also ensures that the constructed tube is flat-foldable. In other words, the tube can be constructed by welding two sheets and folding it up along the center creases (Fig. 05). There also exists a continuous folding motion, which is discussed later.

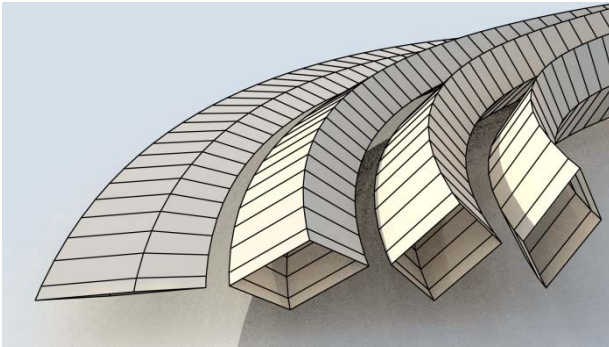


Fig. 05. Flattening the tube.

Subsequently, we can construct a tube with arbitrarily scaled widths of $u^*w_L|_{t=0}$ and $v^*w_R|_{t=0}$. Therefore, any of the derived three creases $\mathbf{x}(t)$ with respect to the original curve can be described by the linear combination of two vector functions $\ell_L \mathbf{r}_L(t)$ and $\ell_R \mathbf{r}_R(t)$ as

$$\mathbf{x}(t) = \mathbf{x}_1(t) + u\ell_L(t)\mathbf{r}_L(t) + v\ell_R(t)\mathbf{r}_R(t), \quad (11)$$

where $\mathbf{x}_1(t)$ describes the original curve and u and v are real number parameters. This means that a set of u and v uniquely determines the curve, and the construction sequence can be arbitrarily set as long as the lengths of segments along \mathbf{r}_L sum up to u , and those along \mathbf{r}_R sum up to v (Fig. 06). This makes sure that complex cellular

structures behave exactly in the same manner as the basic quadrangle tube.

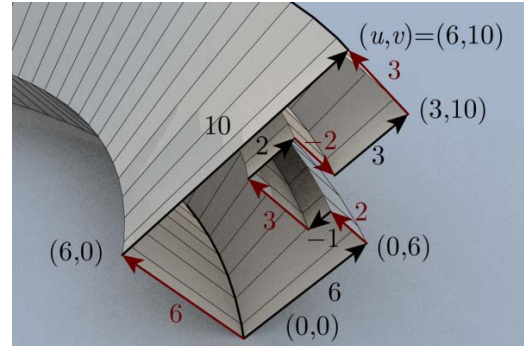


Fig. 06. Derived curve is defined by two parameters u and v (the sequence does not matter).

Width Proportion

From Fig. 03, we can see that the widths between the curves (the distance between the corresponding tangent lines, i.e., $w_{12} = \sin \beta_1 \ell_{12}$) change with respect to the parameter t as a result of the construction method based on parallel tangent vectors. The change in the width is described as

$$\frac{d \ln w_{12}}{dt} = \cot \beta_1 \kappa_{1,2D} \frac{ds_1}{dt} = \frac{\tau_1}{\cot \alpha_1} \frac{ds_1}{dt}, \quad (12)$$

$$\frac{d \ln w_{41}}{dt} = \cot \beta_1 \kappa_{1,2D} \frac{ds_1}{dt} = \frac{-\tau_1}{\cot \alpha_1} \frac{ds_1}{dt}. \quad (13)$$

This implies that a curve with torsion τ of the same sign, e.g., a helix, yields a curved folding with the proportion of w_{12} to w_{41} , increasing or decreasing monotonically with respect to t . An interesting aspect is that the area $A_{1234} = w_{12}w_{41}$ of the section parallelogram is constant with respect to t .

Regression

The construction step of a new curve assumes that it lies within the developable surface. However, because a generic (non-cylindrical) developable surface has either a curve of regression or cone apex, the width $w_R|_{t=0}$ must be set such that $w_R/w_R^{\lim} < 1$, where w_R^{\lim} is the width between the crease and the curve of regression. w_R^{\lim} is calculated as

$$w_R^{\lim} = \frac{(\sin \beta_1)^2}{\frac{\partial \beta_1}{\partial s_1} - \kappa_{2D}}. \quad (14)$$

Similarly,

$$w_L^{\lim} = \frac{(\sin \beta_1)^2}{\frac{\partial \beta_1}{\partial s_1} + \kappa_{2D}}. \quad (15)$$

Thus, the speed functions of the rulings can be represented as follows:

$$\frac{ds_2}{dt} = \left(1 - \frac{w_R}{w_R^{\lim}}\right) \frac{ds_1}{dt}. \quad (16)$$

The linearity can be exploited to obtain a global limit for the cylindrical and cellular structures that can be constructed from a given space curve. Assuming we get a

curve from a sequence of construction steps, which are represented by two parameters u and v in Equation (11), then

$$\frac{ds}{dt} = \left(1 - \frac{uw_L}{w_L^{\text{lim}}} - \frac{vw_R}{w_R^{\text{lim}}}\right) \frac{ds_1}{dt}. \quad (17)$$

This produces a regression line for parameter t .

$$\frac{uw_L}{w_L^{\text{lim}}} + \frac{vw_R}{w_R^{\text{lim}}} = 1. \quad (18)$$

This forms a ruled surface boundary across upon which the space curve cannot lie, thereby defining a domain in the uv space that results in a valid curve.

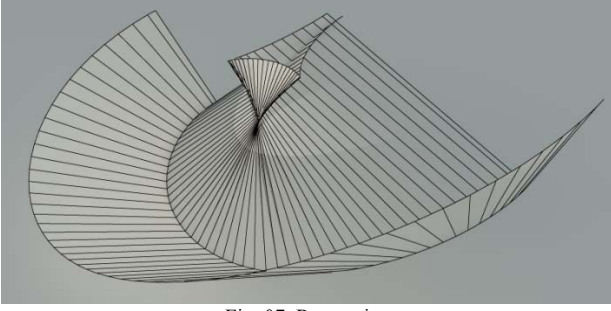


Fig. 07. Regression

KINEMATICS

Single Curved Folding vs. Tube Structure

In general, a curved folding can transform in two ways: folding without a change in the rulings position ($\delta\beta_L = \delta\beta_R = 0$), and twisting with a change in the rulings (Fig. 08). We call former motion “rigid folding” of the curved fold because it is the limit of the rigid folding motion of a discrete quad panel folding as the panels are infinitely subdivided. The latter motion is also a valid motion without stretching of the material and is unique to the smooth curved folding. We can parameterize the configuration using the continuous rulings alignment mappings $S_{0,1}:s_0 \rightarrow s_1$ and $S_{1,2}:s_1 \rightarrow s_2$ between the boundary curves 0 and 2, the crease curve 1, and the folding angle at the start point $\alpha_1(0)$. $S_{i,i+1}$ uniquely determines β_{1L} and β_{1R} and Equations (3) and (4) give a differential equation, through which the folding angle $\alpha(s)$ and torsion $\tau(s)$ are uniquely determined. Any of the variations $\delta S_{0,1}$ and $\delta S_{1,2}$ corresponds to a valid transformation with the change in ruling alignment. Therefore, a curved folding with a single curved crease has excess degrees of freedom and is hard to control its form and motion.

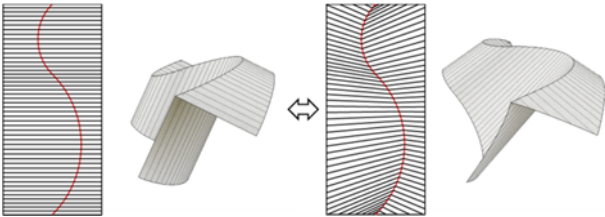


Fig. 08. Folding motion with drifting rulings.

In contrast, the drifting motion can be restricted in the tubular structure. We similarly parameterize the configuration of the tube by ruling alignment $S_{i,i+1}:s_i \rightarrow s_{i+1}$ and $\alpha_i(0)$ ($i = 1, \dots, 4$). However, in this case, the parameters cannot be independently determined because if each crease is separated by adding a cut in the middle of the developable strips connecting the creases, the cut boundary does not match with the adjacent one when $S_{i,i+1}$ and $\alpha_i(0)$ are arbitrarily given. To construct a consistent surface shared by adjacent creases i and $i+1$, the curvature of the surface relative to the speed function s_i and s_{i+1} must be identical: $\left\| \frac{d\mathbf{p}_{i,i+1}}{dt} \right\| = \left\| \frac{d\mathbf{p}_{i+1,i}}{dt} \right\|$, which can be represented as

$$\frac{\kappa_{i,2D} \tan \alpha_i \operatorname{cosec} \beta_{i,i+1}}{\kappa_{i+1,2D} \tan \alpha_{i+1} \operatorname{cosec} \beta_{i+1,i}} \frac{ds_i}{ds_{i+1}} = 1, \quad (19)$$

where $\beta_{i,i+1}$ and $\beta_{i+1,i}$ refer to $\beta_{i,R}$ and $\beta_{i+1,R}$, respectively, if i is odd, and $\beta_{i,L}$ and $\beta_{i+1,L}$, respectively, if i is even.

In addition, to maintain the homeomorphism to a cylinder, the closure condition must be assigned. Assuming that the boundary curves of the tube are kept straight, the boundary follows a sheering motion keeping $\alpha_1(0) = \alpha_2(0) = \alpha_3(0) = \alpha_4(0)$.

To sum up, the motion is parameterized by a single parameter $\alpha_1(0)$ and four variations of the ruling alignment functions $\delta S_{i,i+1}$, which are constrained by four identities given by Equation (19). This implies that in a generic case, there is sufficient number of constraints to stabilize the tube if $\alpha_1(0)$ is fixed. We conjecture that if the boundary curves are straight quads and no cone apex exists on the surface, rigid folding motion will be the only motion available; however, this has not been proven. Here, the former assumption can be realized by reinforcement of the boundary whereas the latter is the result of the physical behavior of a thin elastic sheet that stores an infinite elastic energy at the cone apex.

Tubes Can Rigidly Fold

In a rigid folding motion, intrinsic parameters such as $\kappa_{i,2D}$, $\beta_{i,i+1}$ and $\frac{ds_i}{ds_{i+1}}$ do not change. Therefore, the folding motion with $\delta\alpha_1(t) \equiv \delta\alpha_2(t) \equiv \delta\alpha_3(t) \equiv \delta\alpha_4(t) \equiv \delta\alpha$ satisfies Equation (19). For a given folding angle $2\alpha \in [0, 180^\circ)$, the curve defined by the curvature $\kappa(s) \equiv \frac{\cos \alpha_0(s)}{\cos \alpha(s)} \kappa_0(s)$ and torsion $\tau(s) \equiv \frac{\tan \alpha(s)}{\tan \alpha_0(s)} \tau_0(s)$ is the curve in a folded state, where the original space curve at folding angle $2\alpha_0 \in (0, 180^\circ)$ is defined by the curvature $\kappa_0(s)$ and torsion $\tau_0(s)$.

The cellular structure folds rigidly and flatly in the same manner. This can be visualized as the parallel tangent vectors and tangent planes of the ruled surfaces at a common parameter t orthogonally projected from the common tangent vector, which form a consistent pantograph mechanism.

COMPOSITE DEPLOYABLE VAULT

We show designs of deployable shells using the proposed tubular structures. The basic strategy for the design is to

first construct a tubed arch from a curve and then assemble the arches to form a composite vault.

We design the arch tube such that its boundary quads lie on a common xy plane in a deployed state of $0 < 2\alpha < 180^\circ$, say $2\alpha = 90^\circ$. If this condition is satisfied, the consecutive curves follow the same property and the boundary of the vault is also coplanar. The planarity of each boundary implies that $\beta(0) = \beta(s_1) = 90^\circ$ and thus, $\tau(0) = \tau(s_1) = 0$, where the total length of the curve is denoted by s_1 . The coplanarity of the boundaries, in general, requires the coincidence of four parameters, i.e., $\mathbf{T}(0) - \mathbf{T}(s_1) = \mathbf{0}$ and $(\mathbf{x}(s_1) - \mathbf{x}(0)) \cdot \mathbf{T}(0) = 0$. In general, the tangent vectors and the positions are computed using numerical integration. Here, we show a subset of the design space by assuming reflection symmetry, i.e., $\kappa(s) = \kappa(s_1 - s)$, $\tau(s) = -\tau(s_1 - s)$. In this case, the coplanarity is simplified to

$$\mathbf{T}(0.5s_0) \cdot \mathbf{T}(0) = 0. \quad (20)$$

Typical Design

We built a parametric design system using Grasshopper to calculate the curve, and the tubular and cellular structures. The following shows a typical parametric design example of an assembled vault using space curves of constant curvature and harmonic torsion.

First, the curve is set such that it has constant curvature $\kappa(s) = \kappa_0$ and harmonic torsion $\tau(s) = \alpha\kappa_0 \sin\left(2\pi\frac{s}{s_0}\right)$. We calculate the curve and its frame by discretizing the curve by converting it into a polyline. Then, $\kappa_0 s_0$ is numerically determined using a line search algorithm to satisfy Equation (20). We continue the construction of tubes so that they share the developable creases, i.e., curve 3 of a certain tube is curve 1 of the following tube.

Equations (12) and (13) calculates the change in the width proportion. Owing to the symmetry of the harmonic function, the two end sections share a common proportion $w_R(s_0) = w_R(0)$, and the change in the proportion is the maximum at the middle of the curve as $w_R(0.5s_0) = e^{\frac{1}{\pi}\alpha\kappa_0 s_0} w_R(0)$. Here, the change in the proportion at the middle of the curve is an important design parameter for the resulting vault as the aspect ratio of the rectangular section w_R/w_L at $s = 0$ determines the section feature curve on a horizontal plane (xy plane), whereas the proportion at $s = 0.5s_0$ determines the section feature on a vertical plane (zx plane).

As an example, Fig. 09 shows a vault structure from a curve with $\alpha = 0.3$, in which Equation (20) is satisfied at $\kappa_0 s_0 \approx 3.305$, and thus, the change in the proportion is $\frac{w_R(0.5s_0)}{w_R(0)} \approx 1.37$. We assemble tubes with rectangular sections of aspect ratio $p_{xy} = \frac{w_R(0)}{w_L(0)} = 0.75$ and obtain $p_{xz} = \frac{w_R(0.5s_0)}{w_L(0.5s_0)} = 1.41$ at xz plane.

Fig. 10 shows the design variations obtained by changing parameters $\frac{w_R(0)}{w_L(0)}$ and α . By adjusting these parameters, the slope of the sections at the xy and zx planes can be varied, as seen in Fig. 10.

The structure continuously folds to a flat state. Once the folding angle is varied, the boundary curves do not lie on the ground plane. This is attributed to Bellow's Theorem, which forbids rigidly collapsible, closed polyhedra.

CONCLUSION

In this study, we showed the geometric construction method of curved folded tubular and cellular structures using a space curve. We discussed the folding kinematics of the structure and showed a family of design variations of the deployable vault, by assembling multiple arches. The shape of the assembled vault can be controlled by controlling the amount of total torsion and the proportion of the rectangular section.

ACKNOWLEDGMENT

This work was supported by the JST Presto program.

References

- [1] Tachi, T., "Rigid-Foldable Thick Origami", in *Origami*⁵, pp. 253-263, 2010.
- [2] Tachi, T., Miura, K., "Rigid-Foldable Cylinders and Cells", *Journal of the International Association for Shell and Spatial Structures (IASS)*, 53(4), pp. 217-226, 2012.
- [3] Tachi, T., "One-DOF Rigid Foldable Structures from Space Curves", in *Proceedings of the IABSE-IASS Symposium 2011, London, UK, September 20-23, 2011*.
- [4] Resch R. D., "Portfolio of Shaded Computer Images", *Proc. IEEE*, Vol. 62, No. 4, pp. 496-502, 1974.
- [5] Fuchs D., Tabachnikov S., "More on Paperfolding". *The American Mathematical Monthly*, Vol. 106, No. 1, pp. 27-35, 1999.

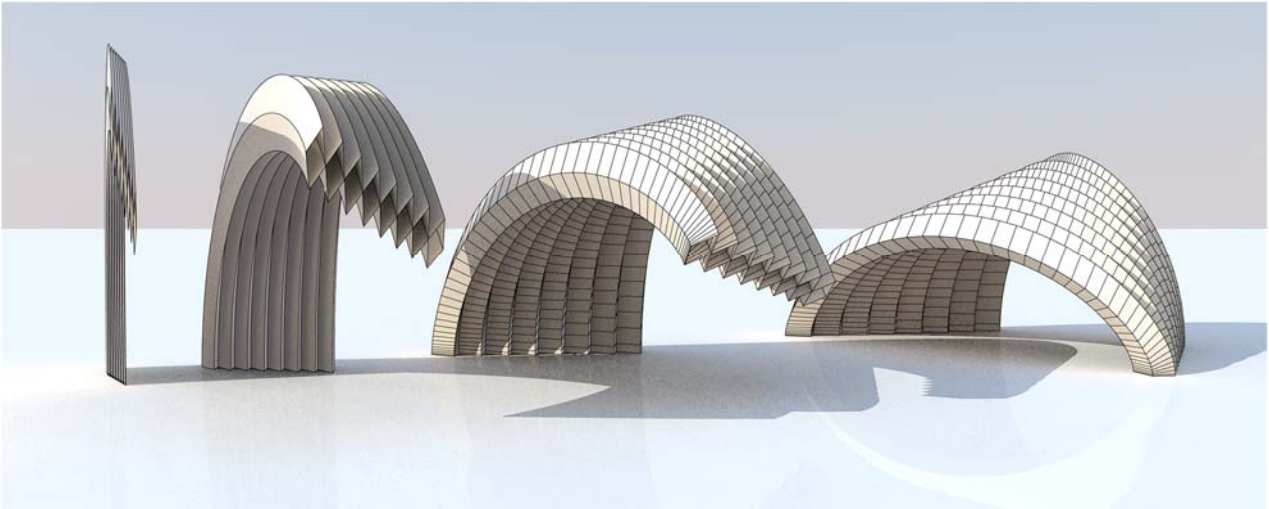


Fig. 09. Folding motion of an example vault constructed form foldable tubes.

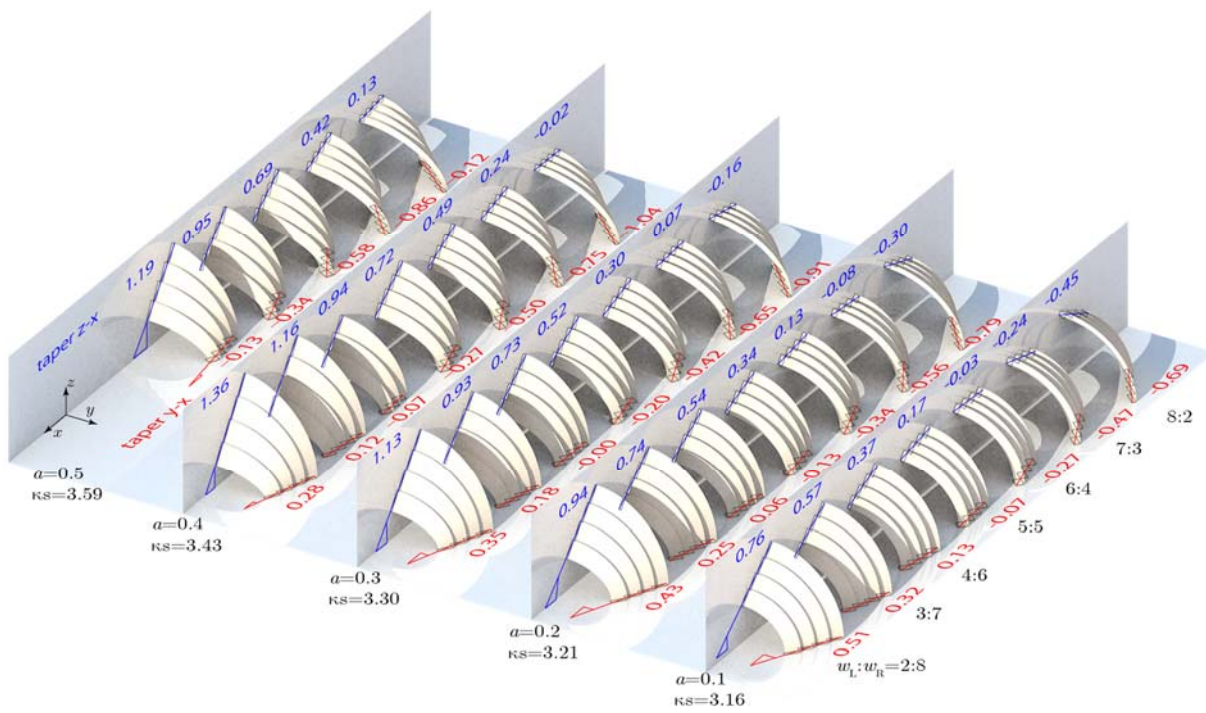


Fig. 10. Variations of the derived form; the slope of the section in the zx plane is indicated in blue and the slope in the xy plane is indicated in red.